DOI: 10.31534/engmod.2026.1.ri.03f
Original scientific paper
Received: 21.04.2026.
This article is an open access article distributed under the terms and conditions of the Creative Commons Attribution (CC BY) license.

Cutting Force Prediction in Turning using Micro-Textured Tools

Shailesh Rao A.(1), **Santosh Kumar**(2), **Suresh Kumar S.**(3), **Sathisha H.M.**(3), **Pavan Kumar B.K.**(4)

(1) *Department of Mechanical Engineering, Nitte (Deemed to be University), Nitte Meenakshi Institute of Technology (NMIT), Bengaluru, INDIA e-mail: shailesh.rao@nmit.ac.in*

(2) *Department of Industrial and Production Engineering, National Institute of Engineering, Mysuru 560008, Karnataka, INDIA*

(3) *Department of Mechanical Engineering, National Institute of Engineering, Mysuru 560008, Karnataka, INDIA*

(4) *Department of Mechanical Engineering, Ballari Institute of Technology and Management, Ballari 583104, Karnataka, INDIA*

SUMMARY

This study investigates the influence of rake-face micro-texturing on turning performance and develops predictive models for cutting force. Turning experiments on AISI 1014 mild steel were performed under four conditions: dry turning (A1), lubricated turning with a plain tool (A2), and lubricated turning with micro-dimple (A3) and micro-channel (A4) textured tools, at two cutting speeds (26 and 39 m/min) and two depths of cut (0.75 and 1 mm). For each test, the cutting force, vibration amplitude, surface roughness and chip saw-tooth distance were measured, while the tool-tip temperature and cutting power were derived from the measured quantities. The micro-channel tool (A4) consistently gave the lowest cutting force, temperature, power consumption and surface roughness, which is attributed to improved lubricant retention at the tool–chip interface. Spearman correlation analysis was used to identify the parameters most strongly associated with the cutting force. Further linear regression models relating the cutting force to input variables such as cutting speed, tool-tip temperature, power and vibration amplitude were developed. Building on the random forest model published in the authors' preliminary study, a factorial analysis of variance and a leave-one-out cross-validated comparison of five machine learning models were then performed. The analysis confirms a statistically significant effect of the tool texture on the cutting force ($p < 0.001$), and multiple linear regression is found to perform best for this dataset ($R^2 = 0.93$, RMSE = 2.85 N), confirming the potential of data-driven models for selecting process parameters and tool texture in turning.

KEY WORDS: *micro-textured tool, turning, cutting force, machine learning.*

1. INTRODUCTION

The development of precise micro-scale patterns on the rake surface of a cutting tool has been reported to improve cutting performance during machining [1-2]. Such textures can take the form of fine ridges, discrete micro-holes or continuous channels, each modifying the tool–chip

contact in a different way. In turning, the geometry of the tool largely determines the quality of the machined component, and the chip formation behaviour, the surface characteristics and the tool wear all change with the tool morphology.

Dry turning is attractive from a cost and sustainability standpoint, since it eliminates the purchase, maintenance and disposal of lubricants and supports clean manufacturing. However, it also enlarges the loaded contact zone at the tool-tip and leads to the generation of residual stresses and surface changes during machining. This has a great effect on the fatigue life and durability of the finished part. Therefore, it is important to predict these effects before the machining process in order to avoid unnecessary costs and material waste [3]. Furthermore, the larger contact area at the tool-tip interface generates more friction and heat that result in an increase in temperature increase and excessive tool wear on the tool's rake and crater surfaces. This wear can lead to chatter and eventually result in a poor-quality machined surface [4].

Lubrication on the tip of a tool reduces friction and improves the flow velocity of the chips over the rake surface of the tool [5]. This leads to a lower temperature in the cutting zone. The contact length under the chip is reduced and the cutting forces are reduced. Another method to improve the machining process is the use of Minimum Quantity Lubrication (MQL) and Minimum Quantity Cooling Lubrication (MQCL) methods, where a small quantity of lubricant (or of a cooled lubricant-air mist) is delivered directly to the cutting zone in a controlled manner. Here, the use of MQL and MQCL helps in cooling the tool-tip junction which results in reduced tool wear and machined surface roughness [6]. Lubrication removes the dissipated heat produced during the machining process and increases the machining efficiency with MQL [7] and MQCL [8] techniques and finally improves the machined surface. The experimental results have demonstrated several advantages of using different lubrication methods over the dry turning process. The supplied liquids also contribute to the enhanced lubricating effect, which results in a lower cutting temperature and a better machining process [9].

The rise in temperature results in reduced tool life and the heat formation develops a residual stress on the machined surface [10]. Even during the lubrication process, there is minimal time for the lubrication to absorb the heat from the tool-tip interface. Hence proper methods of lubrication need to be developed for improving the machining process. Recently, advanced machining techniques, such as tool surface texturing, can help mitigate the effects of friction and heat transfer and improve the tribological properties of the tool during the machining process. This leads to improvements in tool life, surface finish and accuracy of the machined component, as well as a reduction in the environmental impact of the machining process by the proper utilization of coolant [11]. Surface texturing has been shown to improve lubrication in various mechanical components. Researchers have investigated the effect of surface texturing on tools and their behaviour during machining processes. Rao [12] assessed textured and non-textured tools during the machining of mild steel and observed a 30% reduction in the cutting force. Experimental examinations in aluminum alloys have shown that textured tools significantly enhance the machining process, wherein the chip flow direction emerges as a critical factor influencing effectiveness [13]. Furthermore, some studies indicate that perforated carbide tools offer higher performance due to improved lubrication conditions at the tool - chip interface. Micro-hole patterns produced on PCD inserts have similarly improved the machining of titanium alloys [14] and micro-textured tools have been shown to reduce friction, cutting force and stresses at the tool–chip interface in dry cutting [15]. Tool edge wear has been directly linked to increased cutting forces and vibrations during finish machining [16], while chip morphology studies relate serration behaviour to the cutting conditions and to the microstructure of the

machined material [17,18]. The type of cutting fluid applied has also been reported to strongly influence machining performance under MQL conditions [19].

Overall, the micro-perforations on the rake surface of the cutting tools have shown a positive effect in several studies. The cutting parameters such as cutting speed, feed rate, amplitude and cutting forces play a decisive role in determining the machining performance. With the advancement of the data driven techniques such as machine learning, these models have become essential tools for predicting machining responses and optimizing process conditions. In machine learning models, hybrid approaches like the adaptive neuro-fuzzy inference system (ANFIS) can consistently capture nonlinear relationships in machining and help to accurately predict thrust force and surface roughness [20]. The artificial neural network (ANN) based frameworks also provide robust capabilities in machining process optimization, but their performance relies on network structure and parameter selection [21,22]. The neural network models offer unique advantages in obtaining accurate predictions depending on the complexity and dimensionality of machining data [23]. Overall, the above studies indicate that the machine learning modelling with suitable parameter selection helps to improve the prediction of machining outcomes. A detailed methodology, suitable variable parameters and more comprehensive models that generalize across diverse materials and cutting conditions can help achieve more accurate predictions.

The literature reviewed shows that rake-face texturing improves lubrication, reduces friction and extends tool life. Nevertheless, three specific gaps remain. First, a direct comparison of channel-type textures against multiple micro-hole (dimple) textures under otherwise identical turning conditions has received limited attention. Second, most reported studies examine individual responses in isolation, whereas a combined statistical treatment of cutting force, tool-tip temperature, power, vibration amplitude and chip morphology are rarely presented. Third, there is a lack of published research employing machine learning models, such as random forest, to compare tool morphologies and predict the cutting force from measured process data. To address these gaps, the present work (i) fabricates micro-channel and micro-dimple textures on carbide inserts by femtosecond laser micromachining, with the grooves aligned with the chip flow direction to retain lubricant at the tool–chip interface; (ii) experimentally characterises the turning of AISI 1014 steel under dry, lubricated and textured-tool conditions; and (iii) develops correlation, regression and machine learning models to predict the cutting force from the machining parameters. The experimental campaign analysed here is reported in the authors' preliminary study [24], in which a random forest regression and classification framework was developed for the same dataset. The present manuscript substantially extends that work in three respects: an explicit physical comparison of the channel and dimple textures across all measured responses, a factorial analysis of variance quantifying the statistical significance of the texture effect and a leave-one-out cross-validated comparison of five predictive models under a common protocol. No results from the cited literature are reproduced here except where explicitly attributed.

2. EXPERIMENTAL DETAILS

The tests were conducted on a medium duty lathe machine VGM 215 (Balaji make) and the turning process was carried out on AISI 1014 mild steel ($\phi 25 \times 150$ *mm*) using both smooth and texture cutting tools under dry and wet cutting conditions. The turning tool were manufactured from tungsten carbide (WC) containing 10% cobalt (Co) binder of medium toughness grade were employed for machining low carbon steels. The cutting forces were recorded using a CONTECH lathe tool dynamometer (accuracy of 0.1 *N*) that was mounted between the tool holder and the turret. The dynamometer was used to capture the three force components developed during the turning process. The schematic sketch of the lathe machine is shown in Figure 1. The femtosecond laser machining system was used to develop the micro-textures on the rake surface. In the proposed work, two types of textures were generated: Micro-dimples (Figure 2a) and Micro-channels (Figure 2b). The micro-texturing of the carbide inserts was carried out using a femtosecond laser micromachining system (e.g., *Model: Pharos-10W*, *Manufacturer: Light Conversion, Lithuania*). The system has a wavelength of 1030 *nm*, a pulse duration of 200–300 *fs*, an average power of 10 *W* and a spot size of approximately 20–30 μm at the focus. The developed textures consist of micro dimples of approximately 0.5 to 1 *mm* in depth and micro-channels of 0.5 *mm* in width and nearly 1 *mm* in depth.

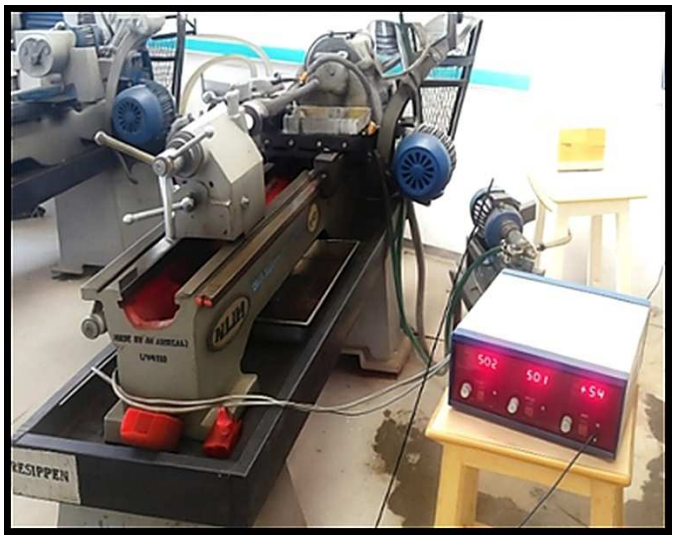


Fig. 1 *Lathe Tool Arrangement with Measurement Instruments*



a) *b)*

Fig. 2 *Perforated Tool with (a) Micro-dimples and (b) Micro-channels*

The machining process was carried out with the different process parameters as depicted in Table 1. Also, the two different cutting speeds (26 and 39 *m/min*) and depths of cut (0.75 and 1 *mm*) were employed for the machining process. During the lubricated tests (A2–A4), a low-viscosity cutting fluid was supplied at a constant flow rate of 40 *cc/hr*. The surface roughness measurement for the machined specimens was carried out using a Mitutoyo Talysurf portable profilometer. The measurements were conducted in accordance with relevant ISO roughness standards, wherein five measurements were taken along different circumferential orientations and the mean roughness value (*Ra*) was computed. The machine tool vibrations were observed using a standard tri-axial accelerometer (frequency range of 0.5–10 *kHz*, sensitivity of approximately 100 *mV/g*) fixed to the tool post. The sensor captured vibration signals in the feed, radial and axial directions. The recorded signals were further fed into an amplifier and data acquisition system for processing and analysis. The force and vibration signals were acquired at a sampling frequency of 25.6 *kHz*, which is more than twice the upper limit of the accelerometer working range (10 *kHz*) and therefore sufficient to prevent aliasing. To obtain the vibration amplitude in terms of displacement (*mm*) reported in Table 2, the acceleration signals were first band-pass filtered (10 *Hz*–5 *kHz*) to remove the DC offset and high-frequency noise, and were then numerically double-integrated in the time domain. The peak amplitude of the resulting displacement signal in the cutting-speed direction was reported. The quantity of heat generated was determined by various factors such as cutting force, rotational speed, and friction at the tooltip. Direct measurement of the tool–chip interface temperature was not feasible in the present set-up, since the contact zone was inaccessible to a contact thermocouple and was shielded from optical (infrared) measurement by the flowing chip. The temperature rise at the tool–workpiece interface, ΔT_c (*℃*), was therefore estimated using the empirical relation given in Eq. (1) [24]. In Eq. (1), P_u is the friction power at the tool-tip (*W*), computed as the product of the measured friction force at the rake face and the chip sliding velocity; M_c is the metal removal rate (*kg/s*), obtained from the selected cutting speed, feed and depth of cut together with the workpiece density; and C_s is the specific heat coefficient of the workpiece material (*Nm/kg*·°C).

$$\Delta T_c = \frac{P_u}{M_c\, C_s} \tag{1}$$

Table 1 *Machining conditions and their designations*

Method	***Process Name***
Dry turning Process	*A1*
Turning process with lubrication	*A2*
Micro drilled textured tool used for machining	*A3*
Micro channel textured tool used for machining	*A4*

Further *R* programming language was used to analyse the relationships among the various machining variables. The graphical representations, regression models and comparative analyses were computed using *R* software to support interpretation of the experimental results. In correlation testing, the Spearman rank correlation coefficient was employed to evaluate the strength and direction of the association between two numeric variables. The correlation coefficient ranges from −1 to 1, where values close to ±1 indicate a strong monotonic relationship and values close to 0 indicate a weak one. The Spearman method was preferred over the Pearson method because it does not assume linearity or normality of the data. For the regression and machine learning models described later, the coefficient of determination (R^2) was used as the measure of goodness of fit.

3. RESULTS

The details of different process parameters and their corresponding values are represented in Table 2. In Table 2, the first two columns (cutting speed and depth of cut) together with the method designation (Table 1) constitute the input (independent) parameters of the experiment, while the remaining columns are the output (dependent) responses. Overall, Table 2 shows that the micro-channel textured tool (A4) showed greater performance for every speed–depth combination. One exception is the cutting power at 39 *m/min* and 1 *mm* depth of cut, where A4 (0.569 *HP*) exceeds A2 and A3; at this highest material removal rate the chips are thicker and may partially clog the channel textures, temporarily reducing the lubrication benefit. Similarly, at 26 *m/min* and 1 *mm* depth of cut the calculated temperature for A3 (102 *°C*) is much higher than for A2 (79 *°C*) and is associated with lower roughness; the dimple texture reduces the tool–chip contact length, which concentrates the friction power over a smaller contact area (raising the local temperature estimate) while simultaneously lowering the friction force and stabilizing chip flow which improves the surface finish. From this, graphical analysis was conducted to understand the relationships among the key machining parameters.

Table 2 *Input machining parameters and corresponding output responses for each turning test*

Cutting Speed (m/min)	*Depth of cut (mm)*	*Tooltip Temperature (^oC)*	*Cutting Force (N)*	*Power (HP)*	*Surface Roughness (μm)*	*Amplitude (mm)*	*Saw Tooth Distance (μm)*	*Method*
26	*1*	*103*	*67*	*0.476*	*9*	*0.2*	*62*	*A1*
26	*1*	*79*	*59*	*0.45*	*8.8*	*0.18*	*52*	*A2*
26	*1*	*102*	*60*	*0.45*	*7.1*	*0.175*	*55*	*A3*
26	*1*	*88*	*55*	*0.432*	*6.8*	*0.17*	*43*	*A4*
26	*0.75*	*88*	*56*	*0.274*	*5.5*	*0.12*	*44*	*A1*
26	*0.75*	*86*	*51*	*0.254*	*5.3*	*0.11*	*33*	*A2*
26	*0.75*	*64*	*49*	*0.225*	*5*	*0.1*	*34*	*A3*
26	*0.75*	*61*	*46*	*0.21*	*4*	*0.09*	*22*	*A4*
39	*1*	*138*	*85*	*0.673*	*8.2*	*0.3*	*74*	*A1*
39	*1*	*120*	*78*	*0.523*	*7.9*	*0.24*	*66*	*A2*
39	*1*	*119*	*77*	*0.512*	*5.8*	*0.27*	*68*	*A3*
39	*1*	*114*	*68*	*0.569*	*4.95*	*0.21*	*59*	*A4*
39	*0.75*	*101*	*67*	*0.4*	*4*	*0.2*	*56*	*A1*
39	*0.75*	*103*	*60*	*0.322*	*3.5*	*0.14*	*49*	*A2*
39	*0.75*	*80*	*61*	*0.255*	*2.85*	*0.17*	*49*	*A3*
39	*0.75*	*72*	*58*	*0.24*	*2.4*	*0.12*	*42*	*A4*

The measured responses are summarised as grouped bar charts in Figure 3. In each panel of Figure 3, the bar colours distinguish the four machining methods A1–A4 defined in Table 1, and the groups on the horizontal axis correspond to the four combinations of cutting speed and depth of cut. From the initial observations, the temperature variations were found to have a significant influence on the machining performance. At elevated temperatures, accelerate tool wear and fluctuations in the cutting forces were observed. Figure 3a establishes that the tool-tip temperature increases with increased depth of cut, keeping other parameters constant. Figure 3b presents the surface roughness values for the different machining conditions. In dry

turning, the absence of lubrication increases the friction at the tool - chip interface resulting in higher thermal loads and finally weakening the cutting edge. Figure 3c explains the change in cutting power for various turning operations and a maximum power reduction of approximately 35% is observed for operations A1 and A3. The vibration measurements were performed using a tri-axial accelerometer and the amplitude in the cutting speed direction was recorded. Here the A1 tool exhibited the highest vibration amplitude, attributed to repetitive loading cycles and reduced stability during machining, as shown in Figure 3d. Figure 3e presents the corresponding chip saw-tooth distances, which follow the same ranking of methods as the vibration amplitude.

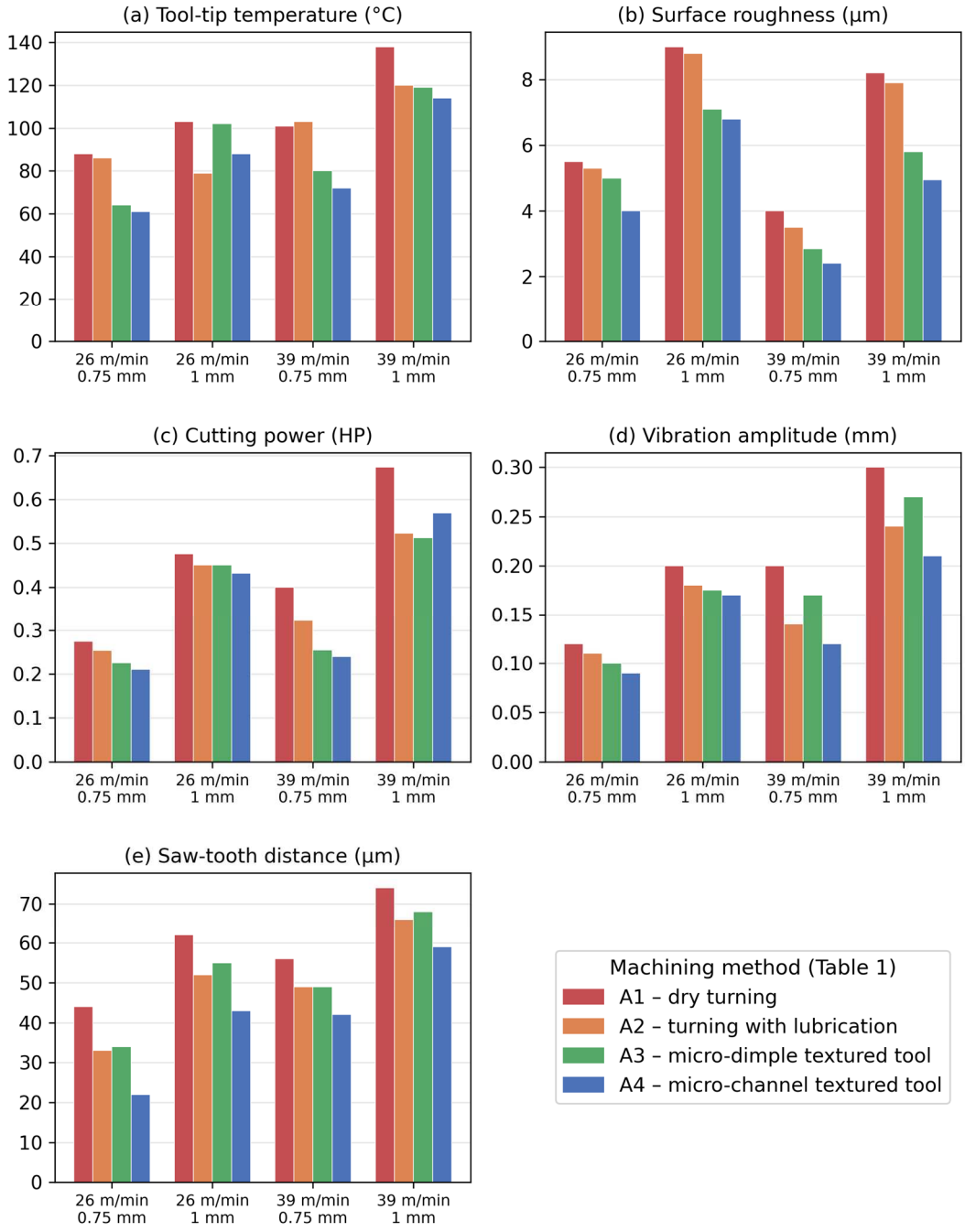


Fig. 3 *Comparison of the measured responses for the four machining methods: (a) tool-tip temperature, (b) surface roughness, (c) cutting power, (d) vibration amplitude and (e) saw-tooth distance*

3.1 CORRELATION AND REGRESSION

Further the correlation values were calculated and presented. Table 3 reports the Spearman correlation coefficients between each pair of variables, computed from the sixteen tests of Table 2 each entry quantifies the strength and direction of the monotonic association between the row and column variables. The cutting force correlates strongly and positively with the tool-tip temperature (0.91) and vibration amplitude (0.95), and moderately with the cutting speed (0.66), indicating that thermal loading and dynamic instability are the dominant companions of high cutting forces. The cutting power is likewise strongly associated with the cutting force (0.85), temperature (0.87) and amplitude (0.91), as expected since power is derived from force and speed. The surface roughness shows only weak-to-moderate correlations with all variables; a weak negative correlation with the cutting speed (−0.36) is observed reflecting the well-known improvement of surface finish at higher speeds, while its strongest association is with power (0.67). The observed moderate-to-strong correlations provided a basis for developing the regression models presented in Section 3.2.

Table 3 *Spearman correlation coefficients between the process variables, computed in R*

	Cutting Speed	***Tool-Tip Temperature***	***Cutting Force***	***Power***	***Surface Roughness***	***Amplitude***
Cutting Force	*0.66*	*0.91*	*1*			
Power	*0.33*	*0.87*	*0.85*	*1*		
Surface Roughness	*-0.36*	*0.45*	*0.41*	*0.67*	*1*	
Amplitude	*0.53*	*0.88*	*0.95*	*0.91*	*0.52*	*1*

3.2 DISCUSSIONS

A comprehensive assessment of the machine responses and the influence of various process parameters on tool performance and product quality was carried out. Further statistical modelling and graphical techniques were employed to evaluate patterns, interactions and variations in the measured variables.

From Figure 3a, during dry turning operations, the tool-tip temperature increases as cutting speed rises. This is due to intensified frictional heating at the tool - chip interface. The temperature and cutting forces are reduced with the application of a low viscosity cutting fluid in the A2 condition that enhances lubrication and heat removal. The tool texturing further influences the temperature reduction due to improved lubricant retention on the rake surface thereby increasing the effective heat radiating area. A higher density of micro - grooves promotes superior heat dissipation during the chip flow where the channel structures help evacuate heat generated during sliding contact. The perforated textures also aid in chip removal and promote the formation of a thin liquid film between the tool - chip interfaces. Figure 3b presents the surface roughness for various machining conditions. The dry turning generates higher surface roughness due to severe frictional heating and weakened tool edge. This induces work hardening on the workpiece surface. The developed hardened surface increased the energy required to shear the chip, thereby increasing the surface roughness values [13]. Under

lubricated conditions, surface roughness diminishes by roughly 35%, and cutting force is reduced by 30% compared to dry cutting. This improvement in surface finish is due to superior interface lubrication and increased tool edge stability. Textured tools further decrease friction by 13–16% and cutting force by 14–20% relative to A1 and A2, leading to a better surface finish. The development of a thin lubricating film across the textured surface reduces frictional resistance, shear stress, and von Mises stress at the tool – chip interface [25].

The machining power increases within the A1 condition at elevated spindle speeds, due to increased friction and the necessity of penetrating the hardened surface of the workpiece, as illustrated in Figure 3c. Dry turning shows the greatest energy utilization due to higher inertia forces and thermal stresses. Power consumption decreases progressively from A2 to A4 with textured tools enhancing tool workpiece adhesion and forming a stable lubricating film. For perforated (A4) tools, improved lubrication within the cutting zone yields the lowest power consumption across the evaluated conditions. The vibration features of the A1 condition are characterized by the highest amplitude, stemming from thermal degradation of the tool-tip and unstable cutting cycles. In this instance, tool flank wear at elevated temperatures fosters instability, which in turn amplifies vibration amplitude. Lubrication serves to reduce both flank wear and vibration amplitude, and micro-holes within textured tools contribute to reduced friction and improved dynamic stability, as demonstrated by Fang [26]. The textured inserts (A3 and A4) reduce the self-excited vibrations and chatter during the turning process due to enhanced adhesion, reduced cutting temperature and improved tribological conditions at the tool–chip interface. This results in improved machining quality and extended tool life. Also, the chip morphology exhibits significant variation depending on the machining conditions. With reduced cutting speeds and in dry turning scenarios, oscillations at the tool–chip contact interface give rise to irregular serrated chips and increased surface roughness. Conversely, an increase in cutting speed leads to a greater serration pitch, a consequence of dynamic chip formation behaviour. Machining at a cutting speed of 26 *m/min* and a 1 *mm* depth of cut results in larger serrations, a consequence of increased heat generation, thermal softening, and inadequate heat dissipation. For untextured tools, higher speeds contribute to increased serration height due to augmented friction and thermal accumulation on the rake surface. Conversely, the lubricated conditions reduces the chip waviness. Enhanced lubrication leads to reduced serration length and less tool wear. Textured tools facilitate continuous chip formation with minimal waviness, likely attributable to a thin liquid coating on the rake surface that stabilizes chip flow. Furthermore, at elevated cutting speeds, textured tools decrease chip thickness, suggesting an increased shear angle and a more stable cutting process.

Differences in how chips form with textured and untextured tools arise from the microscopic structure of the material being worked on. Removing carbides, oxides, and non-metallic inclusions requires more shear force, which generates significant heat and stress at the tool's cutting edge [12]. This leads to wear and unusual serration patterns. Additionally, dry turning increases the likelihood of burr formation because of increased friction, which is consistent with the findings of Surjeet [27]. The wear caused by micro-welded chips is more pronounced at the high speeds in dry turning process. Tools with surface textures produce continuous chips characterized by reduced serration and minimal burr development. At elevated cutting speeds, the shorter contact duration between the tool and the workpiece increases the serration spacing, whereas at lower speeds, enhanced heat dissipation reduces serration thickness. In summation, the incorporation of lubrication and tool texturing demonstrably improves thermal management, reduces cutting forces, stabilizes chip formation and extends tool lifespan relative to traditional dry turning.

Further, in this study, a regression analysis was carried out to investigate the relationship between dependent and independent variables, based on the moderate correlations found in the correlation table. Specifically, the following relationships were investigated:

1. The relationship between cutting speed and tool-tip temperature, and their impact on cutting force.
2. The relationship between amplitude and power, and their effect on cutting force.

Here, the *R* programming tool was used to develop models for cutting force and cutting tool-tip temperature based on other input parameters. The results of the regression analysis for the cutting force and tool-tip temperature models are presented below:

- Cutting force = 11.857 + (0.39 x cutting speed) + (0.395 x tool-tip temperature) **(2)**
- Cutting force = 32.868 – (14.84 x power) + (201.82 x amplitude) **(3)**

The cutting force was selected as the modelled quantity as it is the principal indicator of machinability in turning that governs the cutting power and the vibration amplitude, drives tool wear, and directly reflects the effectiveness of lubrication and tool texturing. In Eq. (2) and Eq. (3) the cutting force is obtained in *N*, with the cutting speed in *m/min*, the tool-tip temperature in *°C*, the power in HP and the vibration amplitude in mm; the regression coefficients accordingly carry the corresponding reciprocal units. The two expressions are complementary rather than interchangeable. Eq. (2) estimates the cutting force from the process setting and the thermal state (cutting speed and the tool-tip temperature estimated from Eq. (1)) and is intended for pre-process prediction, whereas Eq. (3) relates the force to the measured dynamic responses (power and vibration amplitude) and is applicable to in-process monitoring. Over the sixteen experiments, the two models achieved R^2 values of 0.88 and 0.93, respectively (Figure 4).

The random forest, a machine learning model introduced by Breiman [28], uses a bagging approach over multiple decision trees to enhance predictive performance. A random forest model for this dataset was first reported in the authors' preliminary study, where the model was re-implemented with the cutting force as the output variable and only the true input features (cutting speed, tool-tip temperature, power and vibration amplitude), as an enhancement of the two regression models described above. To optimize the algorithm for the given dataset, the number of trees (ntree) was varied using the trial-and-error method, and a forest of 300 trees was found to produce the best results, matching the accuracy reported (*RMSE* of 0.812 *N* and R^2 of 0.89).

When comparing the predicted and actual trend line, the scatter points are closely aligned with the trend line, indicating that the model predicts the cutting force accurately over the tested range of process parameters. The two graphs in Figure 4 were generated by applying the regression models in Eq. (2) and Eq. (3) to the sixteen experiments: Figure 4a plots the measured cutting force against the values predicted by Eq. (2) (R^2 = 0.88), and Figure 4b plots the measured cutting force against those predicted by Eq. (3) (R^2 = 0.93), together with the fitted trend line and the ideal line in each case.

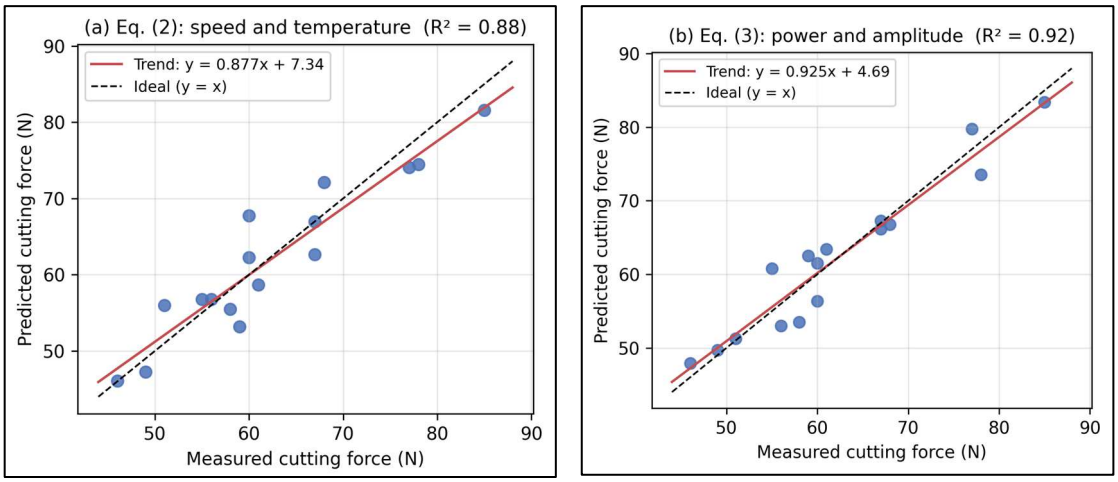


Fig. 4 *Measured versus predicted cutting force over the sixteen turning tests, obtained using (a) the regression model in Eq. (2) and (b) the regression model in Eq. (3)*

Figure 5a illustrates the convergence of the out-of-bag *RMSE* with the number of trees; the error stabilises well before 300 trees, confirming that the chosen forest size is adequate. For practical purposes it is essential to identify the variables that most influence the prediction, and the random forest feature importance index was used for this purpose. As shown in Figure 5b, the vibration amplitude is by far the most influential input, followed by the tool-tip temperature and the power, while the cutting speed has the least influence on the prediction once the thermal and dynamic responses are taken into account. This ordering is consistent with the correlation analysis presented in Table 3 (amplitude–force 0.95, temperature–force 0.91) and differs from the importance ranking reported earlier, where the output responses themselves were included among the ranked features. In addition to the cutting force, the vibration amplitude and power were also critical parameters. Although the depth of cut is a critical parameter, it was varied over only two levels in the experiments and its influence was largely captured through the derived power and temperature. Therefore, it was not included as a separate input in the modelling process. In the case of the saw-tooth distance, the correlation with the cutting force was not satisfactory, and it was therefore not considered as an input variable in the model.

Overall, the figure presents the relative importance index, offering useful insights into the critical variables that influence the machining process under different tool conditions.

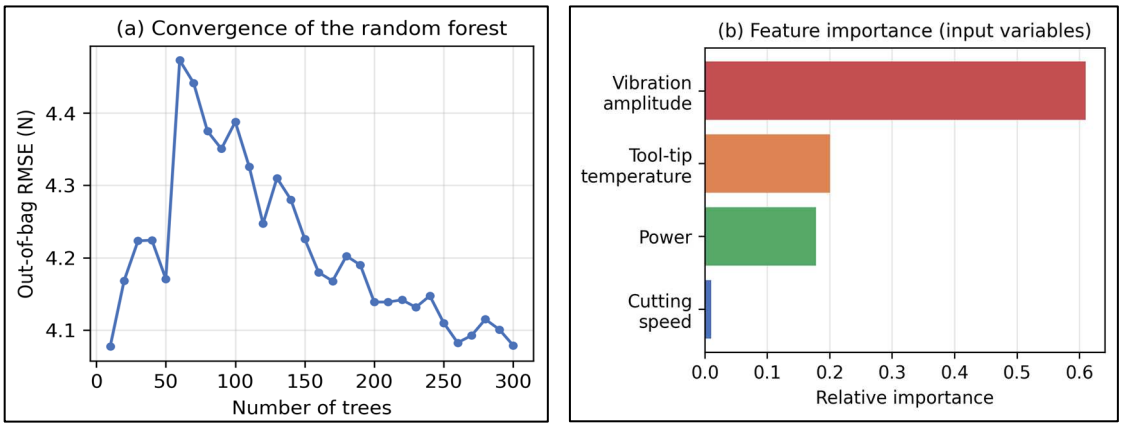


Fig. 5 *Results of the re-implemented random forest model: (a) convergence of the out-of-bag RMSE with the number of trees and (b) relative importance of the four input variables*

3.3 ANALYSIS OF VARIANCE AND COMPARISON OF MACHINE LEARNING MODELS

To complement the correlation analysis, a factorial analysis of variance (ANOVA) was performed on the measured cutting force, treating the cutting speed (two levels), the depth of cut (two levels) and the machining method A1–A4 (four levels) as factors. Table 4 summarizes the results. All three main effects are statistically significant at the 5% level. The cutting speed accounts for 43.8% of the total variation in the cutting force (F = 251.5, p < 0.001) while the depth of cut account for 36.2% (F = 208.2, p < 0.001). The machining method, representing the presence and type of texturing and lubrication, accounts for a further 16.6% of the variation (F = 31.7, p < 0.001). The speed–depth interaction is small but significant (1.9%, p = 0.009), and the residual variation is only 1.6%. The ANOVA therefore confirms that the choice of tool texture has a statistically significant effect on the cutting force in addition to the influence of the process settings.

Table 4 *Factorial ANOVA of the measured cutting force*

Source	*SS (N^2)*	*df*	*MS*	*F*	*p*	*C (%)*
Cutting speed	*770.1*	*1*	*770.1*	*251.5*	*< 0.001*	*43.8*
Depth of cut	*637.6*	*1*	*637.6*	*208.2*	*< 0.001*	*36.2*
Method (A1–A4)	*291.2*	*3*	*97.1*	*31.7*	*< 0.001*	*16.6*
Speed × depth	*33.1*	*1*	*33.1*	*10.8*	*0.009*	*1.9*
Residual	*27.6*	*9*	*3.1*	–	–	*1.6*
Total	*1759.6*	*15*	–	–	–	*100*

In addition to the random forest model of Section 3.2, four further machine learning models were trained to predict the cutting force from the same input features (cutting speed, tool-tip temperature, power and vibration amplitude): multiple linear regression, k-nearest neighbors (k = 3), support vector regression with a radial basis function (*RBF*) kernel, and gradient boosting. Because the dataset comprises sixteen experiments, leave-one-out cross-validation (LOOCV) was adopted for the comparison: each model was trained sixteen times on fifteen tests and evaluated on the withheld test, so that every prediction was made on unseen data. Table 5 reports the resulting root mean square error (*RMSE*), mean absolute error (*MAE*) and R^2, and Figure 6 plots the cross-validated predictions against the measured cutting force. Multiple linear regression performed best (R^2 = 0.93, *RMSE* = 2.85 *N*), which is consistent with the strong monotonic correlations reported in Table 3, followed by gradient boosting (R^2 = 0.86) and random forest (R^2 = 0.84). The distance-based k-nearest neighbors (R^2 = 0.77) and support vector regression (R^2 = 0.68) were less suited to such a small sample. The LOOCV figures are more conservative than the single-split estimate reported in Section 3.2 because every experiment is predicted while held out of training. The feature importance indices of the tree-based models agree with the correlation analysis, ranking the vibration amplitude and the tool-tip temperature as the most influential predictors. These results indicate that, for datasets of this size, the simpler regression model remains the most reliable predictor, while the ensemble methods confirm the robustness of the identified parameter influences; a larger experimental campaign would allow the nonlinear models to demostrate their full advantage.

Table 5 *Leave-one-out cross-validated performance of the machine learning models for cutting force prediction*

Model	***RMSE (N)***	***MAE (N)***	***R^2***
Multiple linear regression	*2.85*	*2.57*	*0.93*
Gradient boosting (300 trees)	*3.93*	*3.25*	*0.86*
Random forest (300 trees)	*4.21*	*3.42*	*0.84*
k-nearest neighbours (k = 3)	*5.03*	*3.79*	*0.77*
Support vector regression (RBF)	*5.92*	*4.45*	*0.68*

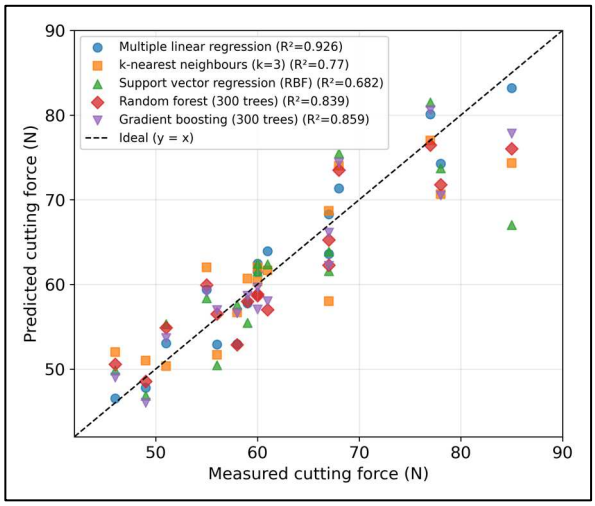


Fig 6 *Leave-one-out cross-validated predictions of the cutting force for the five machine learning models, plotted against the measured values*

4. CONCLUSIONS

The present study examined the influence of microtextured cutting tools, machining parameters and lubrication on turning performance. Further, the integrated statistical and machine-learning models were developed to establish predictive relationships among key machining responses. From this, the following conclusions can be made

- The micro texturing on the rake face, particularly the micro-channel design (A4) showed superior thermal and tribological performance. The channel type textures improve the lubricant retention and increase the effective heat dissipation area, resulting in reduced tool-tip temperature. In this case, an improved thermal condition contributed to lower cutting forces, reduced vibration amplitude and improved surface finish. Further, continuous chips with reduced serration and minimal burr formation were obtained compared to dry cutting, and the untextured tool (A1) formed chips with more pronounced serration and burr formation. The power consumption was lowest for the A4 process due to reduced frictional

resistance at the tool - chip interface. The statistical correlation analysis showed moderate to strong associations among cutting speed, tool-tip temperature, power and vibration amplitude with cutting force. The linear regression models developed confirmed these relationships by achieving R^2 values between 0.88 and 0.92 indicating increased predictive capability. A random forest model, first reported for this dataset in the authors' preliminary study [25], was re-implemented using only the four input variables to understand the nonlinear relationships among the process parameters, reproducing the published accuracy (R^2 = 0.89, $RMSE$ = 0.812 N) on an 80:20 split. Its feature importance analysis ranked the vibration amplitude as the most significant predictor of the cutting force, followed by the tool-tip temperature and power, consistent with the correlation analysis. These findings underscore the critical roles of both thermal and dynamic stability in achieving precise predictions and effective control of machining performance.

- A factorial analysis of variance confirmed that, in addition to the cutting speed (43.8% contribution) and depth of cut (36.2%), the machining method, representing the presence and type of rake-face texturing, has a statistically significant effect on the cutting force (16.6%, $p < 0.001$). A leave-one-out cross-validated comparison of five machine learning models further showed that multiple linear regression performed best on the present dataset (R^2 = 0.93, $RMSE$ = 2.85 N), followed by gradient boosting (R^2 = 0.86) and random forest (R^2 = 0.84), indicating that simple regression models remain highly competitive for small, well-structured machining datasets. At the same time, ensemble methods corroborate the identified parameter influences.

5. REFERENCES

[1] Agari, S.R., Wear and surface characteristics on tool performance with CVD coating of Al_2O_3/TiCN inserts during machining of Inconel 718 alloys, *Archive of Mechanical Engineering*, 69(1), pp. 59–75, 2021. https://doi.org/10.24425/ame.2021.139647

[2] Mishra, S.K., J.I., Ghosh, S. and Aravindan, S., State-of-the-art research and corresponding industrial perspective for the use of textured surfaces in machining applications, *Journal of Micromanufacturing*, 9(1), pp. 131-180, 2025.

https://doi.org/10.1177/25165984241301537

[3] Krolczyk, G.M., Maruda, R.W., Krolczyk, J.B., Wojciechowski, S., Mia, M., Nieslony, P. and Budzik, G., Ecological trends in machining as a key factor in sustainable production – a review, *Journal of Cleaner Production*, 218, pp. 601–615, 2019.

https://doi.org/10.1016/j.jclepro.2019.02.017

[4] Rinaldi, S., Umbrello, D., Rotella, G. and Del Prete, A., A Physically Based Model to Predict Microstructural Modifications in Inconel 718 High Speed Machining, *Procedia Manufacturing*, 47 (January), pp. 487–492, 2020.

https://doi.org/10.1016/j.promfg.2020.04.344

[5] Fan, W., Ji, W., Wang, L., Zheng, L. and Wang, Y., A review on cutting tool technology in machining of Ni-based super alloys, *The International Journal of Advanced Manufacturing Technology*, 110, pp. 2863–2879, 2020.

https://doi.org/10.1007/s00170-020-06052-9

[6] Behera, B.C., Ghosh, S. and Rao, P.V., Modeling of cutting force in MQL machining environment considering chip–tool contact friction, *Tribology International*, 117, pp. 283–289, 2018. https://doi.org/10.1016/j.triboint.2017.09.015

[7] Rao, A.S., Effect of nose radius on the chip morphology, cutting force and tool wear during dry turning of Inconel 718, *Tribology – Materials, Surfaces & Interfaces*, 17(1), pp. 62–71, 2023. https://doi.org/10.1080/17515831.2022.2160161

[8] Maruda, R.W., Krolczyk, G.M., Wojciechowski, S., Zak, K., Habrat, W. and Nieslony, P., Effects of extreme pressure and anti-wear additives on surface topography and tool wear during MQCL turning of AISI 1045 steel, *Journal of Mechanical Science and Technology*, 32, pp. 1585–1591, 2018. https://doi.org/10.1007/s12206-018-0313-7

[9] Chetan, Behera, B.C., Ghosh, S. and Rao, P.V., Wear behavior of PVD TiN coated carbide inserts during machining of Nimonic 90 and Ti6Al4V superalloys under dry and MQL conditions, *Ceramics International*, 42(13), pp. 14873–14885, 2016.

https://doi.org/10.1016/j.ceramint.2016.06.124

[10] König, W, Fritsch, R., Kammermeier, D., New approaches to characterizing the performance of coated cutting tools, *CIRP Annals*, 41(1), pp. 49-54, 1992.

https://doi.org/10.1016/S0007-8506(07)61150-0

[11] Radhika, A., Shailesh Rao, A. and Yogesh, K.B., Evaluating machining performance of AISI 1014 steel using gingelly oil as cutting fluid, *Australian Journal of Mechanical Engineering*, 19(4), pp. 445–456, 2019. https://doi.org/10.1080/14484846.2019.1636517

[12] Agari, S.R., Lakshmikanthan, A., Selvan, C.P., and Vijay Sekar, K.S., Improvement in the machining processes by micro-textured tools during the turning process, *Engineering Proceedings*, 61(1), 2024. https://doi.org/10.3390/engproc2024061002

[13] Rao, C.M., Rao, S.S. and Herbert, M.A., Development of novel cutting tool with a micro-hole pattern on PCD insert in the machining of titanium alloy, *Journal of Manufacturing Processes*, 36, pp. 93–103, 2018. https://doi.org/10.1016/j.jmapro.2018.09.028

[14] Li, Q., Pan, C., Jiao, Y. and Hu, K., Investigation on cutting performance of micro-textured cutting tools, *Micromachines*, 10(6), pp. 352, 2019.

https://doi.org/10.3390/mi10060352

[15] Jesudass Thomas, S. and Kalaichelvan, K., Comparative study of the effect of surface texturing on cutting tool in dry cutting, Materials and Manufacturing Processes, 33(6), pp. 683–694, 2018. https://doi.org/10.1080/10426914.2017.1376070

[16] Chen, G., Wang, J., Xu, J., Han, Z., Yu, H. and Ren, L.Q., Effect of Forward and Reverse Cutting on Tool Wear Behavior in Ultrasonic Vibration-assisted Milling of 3D Needle-punched C/SiC Composites, *Wear*, 552–553 (June), 205454, 2024.

https://doi.org/10.1016/j.wear.2024.205454

[17] Zhao, Z., To, S. and Zhuang, Z., Serrated Chips Formation in Micro Orthogonal Cutting of Ti6Al4V Alloys with Equiaxial and Martensitic Microstructures, *Micromachines*, 10(3), 197, 2019. https://doi.org/10.3390/mi10030197

[18] Mašek, P., Alagan, N.T., Mára, V., Awe, S.A., Nwabuisi, E. and Zeman, P., Chip Formation and Morphology in Cryogenic Machining of Al-SiC Composites, *The International Journal of Advanced Manufacturing Technology*, 137 (5–6), 2899–2917, 2025.

https://doi.org/10.1007/s00170-025-15337-w

[19] Chen, S., Yan, P., Zhu, J., Wang, Y., Zhao, W., Jiao, L. and Wang, X., Effect of Cutting Fluid on Machined Surface Integrity and Corrosion Property of Nickel Based Superalloy, *Materials* 16(2), 843, 2023. https://doi.org/10.3390/ma16020843

[20] Vicente-García, L., Santos-Martín, F., Merino-Gómez, E. and San-Juan, M., Neuro-fuzzy Optimization of Cutting Tool Geometry in Machining Using Sugeno and Mamdani

Inference Models, *The International Journal of Advanced Manufacturing Technology*, October, 2025. https://doi.org/10.1007/s00170-025-16742-x

[21] Sondagar, H., Bhadauria, S.S. and Sharma, V.S., Artificial Neural Network (ANN) Based Prediction of Process Parameters in Additive Manufacturing, *IOP Conference Series Materials Science and Engineering*, 1136 (1), 012026, 2021.

https://doi.org/10.1088/1757-899x/1136/1/012026

[22] Vendittoli, V., Polini, W., Walter, M.S.J. and Geißelsöder, S., Introducing Artificial Neural Networks to Predict the Dimensional and Micro-geometrical Deviations of Additively Manufactured Parts, *Procedia CIRP*, 129 (January), 181–86, 2024.

https://doi.org/10.1016/j.procir.2024.10.032

[23] Dewangan, S.K., Jain, S., Lee, H., Youn, G., Jain, R., Baghel, V.S., Mohan, M., et al., Neural Network-enabled Prediction and Optimization of Mechanical Properties and Biocompatibility in High-entropy Alloys: A Data-driven Approach to Metallurgical Innovation, *Journal of Materials Research and Technology*, 42 (April), 3313–3329, 2026. https://doi.org/10.1016/j.jmrt.2026.04.026

[24] Rao, S.A., Kumar, S., Kumar, S.S., Sathisha, H.M. and Kumar, P.B.K., Improving turning machining processes through integration of micro-textured tools: a modeling approach, *AIUB Journal of Science and Engineering*, 24(2), pp. 135–140, 2026.

https://doi.org/10.53799/1wrpgg16

[25] Bharath, H. and Venkatesan, K., Comprehensive Review of the Micro-texture in Turning Applications: Current State and Recent Advancements, *Advances in Materials and Processing Technologies*, 11 (4), 3704–3800, 2025.

https://doi.org/10.1080/2374068x.2025.2559957

[26] Fang, N., Pai, P.S. and Mosquera, S., Effect of tool edge wear on the cutting forces and vibrations in high-speed finish machining of Inconel 718: an experimental study and wavelet transform analysis, *The International Journal of Advanced Manufacturing Technology*, 52(1–4), pp. 65–77, 2011. https://doi.org/10.1007/s00170-010-2703-6

[27] Davim, J.P., Sreejith, P.S., Gomes, R. and Peixoto, C, Experimental Studies on Drilling of Aluminium (AA1050) Under Dry, Minimum Quantity of Lubricant, and Flood-lubricated Conditions, *Proceedings of the Institution of Mechanical Engineers, Part B: Journal of Engineering Manufacture*, 220(10), 1605-1611, 2026.

https://doi.org/10.1243/09544054JEM557

[28] Breiman, L., Random forests, *Machine Learning*, 45(1), pp. 5–32, 2001.

https://doi.org/10.1023/A:1010933404324